Chemistry & Biology
Article

Switching Heterotrimeric G Protein Subunits with a Chemical Dimerizer

Mateusz Putyrski[1] and Carsten Schultz[1,*]
[1]Cell Biology and Biophysics Unit, European Molecular Biology Laboratory, Meyerhofstr. 1, 69117 Heidelberg, Germany
*Correspondence: schultz@embl.de
DOI 10.1016/j.chembiol.2011.07.013

SUMMARY

The selective manipulation of single intracellular-signaling events remains one of the key tasks when studying signaling networks. Here, we demonstrate for the first time the stimulation of FKBP fusions of various subunits of heterotrimeric G proteins by the simple addition of the chemical dimerizer rapamycin. Activation of constitutively active $G\alpha_q$, but not its GDP-bound form, leads to sustained oscillations of intracellular calcium and *myo*-inositol 1,4,5-trisphosphate ($InsP_3$) levels in HEK cells, independent of the activation of endogenous $G\alpha_q$, in full agreement with the $InsP_3$-Ca^{2+} cross-coupling model of calcium oscillations. Rapamycin-induced translocation of wild-type $G\alpha_s$ to the plasma membrane results in elevated cAMP levels. Activation of rapamycin-inducible $G\alpha_s$ or $G\beta_1\gamma_2$ evokes extensive modulation of ATP-induced calcium transients. The results demonstrate that inducible heterotrimeric G protein subunits will provide ways for dissecting G protein-coupled receptor signaling.

INTRODUCTION

For the understanding of intracellular signaling networks, it is mandatory to dissect single signaling components not only biochemically in artificial systems but also in the living cell. Although overexpression of genes or the use of siRNAs might be suitable for elevating or reducing the level of almost any protein of the genome, their application is comparably slow, and the outcome may be obscured by compensatory mechanisms. Small molecules act usually much faster in this respect. However, most pharmacological approaches will target receptors, thereby activating or inhibiting entire signaling modules. On the other hand, inhibitors acting downstream of the receptor level will usually block only a single branch of the signaling network, leaving the rest of the network intact with all its complexity. In contrast the use of specific activators appears to be a promising way of dissecting signaling networks. Naturally, specific activators are hard to come by, although membrane-permeant derivatives of intracellular messengers (Subramanian et al., 2010; Laketa et al., 2009; Schultz et al., 1993) and natural compounds such as forskolin fall into this category. Furthermore, analog-sensitive kinase alleles hold great promise for dissecting kinome networks (Shokat and Velleca, 2002). Other alternatives are switchable proteins, preferentially those switched by light (Karginov et al., 2010; Janovjak et al., 2010; Wu et al., 2009). Although there are a few prominent examples for the latter, their preparation and use are still in their infancy. More accessible are enzyme constructs that are switchable by changing their location (Suh et al., 2006; Varnai et al., 2006; Szentpetery et al., 2010; Fili et al., 2006; Inoue et al., 2005). This is achieved by fusing the binding domain of a chemical dimerizer such as rapamycin to the protein of interest and locating the orthogonal rapamycin-binding domain to the region where enzyme activity is transferable to the effector molecules. This strategy has been very successfully applied to lipid phosphatases and kinases that will find their substrate only at the plasma membrane (Suh et al., 2006; Varnai et al., 2006). In general a constitutively active form is expressed in the cytoplasm as a fusion to FKBP, whereas the partner domain (FRB) is equipped with a targeting sequence that ensures lipidation. Other examples include manipulation of phosphoinositide levels in Golgi membranes (Szentpetery et al., 2010) and early endosomes (Fili et al., 2006), translocation of small GTPases such as RhoA or Cdc42 (Inoue et al., 2005), or receptor occupancy-independent activation of β-arrestins (Terrillon and Bouvier, 2004).

Here, for the first time we expand this technique to heterotrimeric G protein subunits. Receptor activation usually triggers several different signaling entities simultaneously (Figure 1A), typically more than one of the Gα forms ($G\alpha_q$, $G\alpha_s$, $G\alpha_{12/13}$, and $G\alpha_i$) and, invariably, the Gβγ heterodimers (Wettschureck and Offermanns, 2005). So far, it is difficult to determine the contribution of each of these components to the signaling network. With the help of the rapamycin-induced specific activation of single G protein isoforms (Figure 1B), the effect of each of them could be studied separately, independently of other isoforms, Gβγ dimer activity, and modulation on the receptor level. As an example, the anticipated mechanism of action of the inducible $G\alpha_q$ is depicted in Figure 1C. We chose to assess the effect of the designed constructs by monitoring the levels of secondary messengers: intracellular calcium ($[Ca^{2+}]_i$, monitored by the fluorescent indicator Fluo-4) and cyclic AMP (cAMP, monitored by an Epac-based FRET sensor developed in the lab of K. Jalink; Ponsioen et al. [2004]).

RESULTS AND DISCUSSION

Design of the Inducible Constructs

We prepared mRFP-FKBP fusion constructs for human $G\alpha_q$ with various linkers between FKBP and the Gα protein (see Table S1

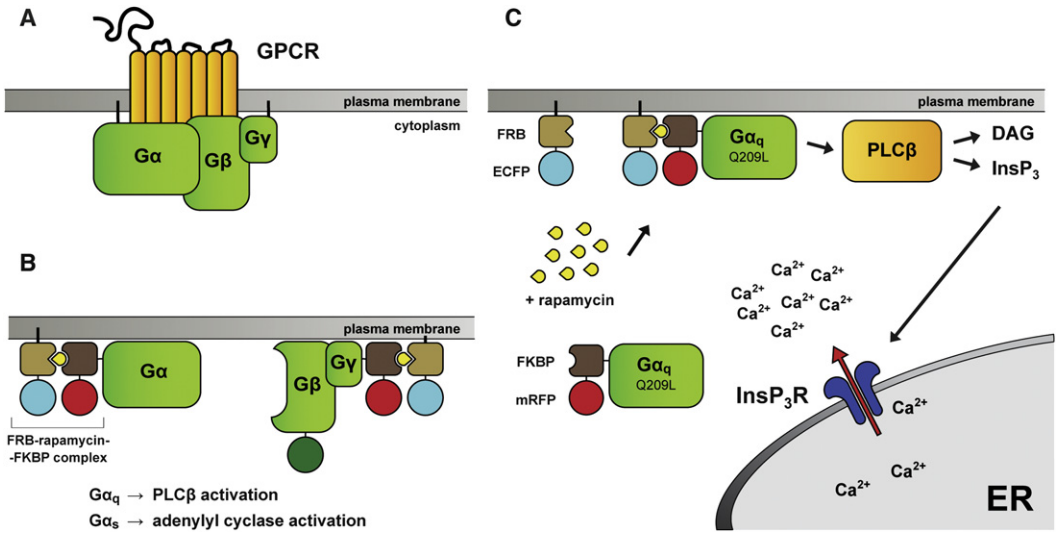

Figure 1. Rapamycin-Inducible Heterotrimeric G Proteins

(A) Ligand binding to G protein-coupled receptors (GPCR) simultaneously activates heterotrimeric G proteins: Gα subunits and the Gβγ heterodimer.

(B) To independently activate each of the G proteins in the absence of receptor activation, cytoplasmic fusion proteins are translocated to the plasma membrane by addition of rapamycin.

(C) Translocation of a GTPase-deficient mutant of $G\alpha_q$ activates PLCβ to generate $InsP_3$ and diacylglycerol (DAG) from $PtdInsP_2$. $InsP_3$ induces calcium release from internal stores. ER, endoplasmic reticulum.

See also Figure S1.

available online) in which the innate palmitoylation residues C9 and C10 of $G\alpha_q$ were replaced by serines to prevent interaction with the plasma membrane and, hence, with the target phospholipase Cβ (PLCβ). Interestingly, only the construct with a lysine-rich linker was ultimately successful in elevating $[Ca^{2+}]_i$. However, an analogous construct design was applied to $G\alpha_s$ without an N-terminal Cys to Ser mutation in the $G\alpha_s$ portion. For both Gα isoforms two variants of the FKBP fusions were created: a wild-type (WT); and a constitutively active, GTPase-deficient mutant (Waldo et al., 2010). Activity was induced by artificially targeting the G protein fusions to the rapamycin-binding FRB domain located at the plasma membrane. The FRB domain was equipped with an Lck N-terminal palmitoylation sequence for plasma membrane targeting and was additionally tagged with ECFP or its nonfluorescent mutant ECFP W66A. These constructs permitted plasma membrane translocation of the FKBP fusions within 10–30 s after addition of rapamycin (Figures S1A, S1B, and S2). Half-maximal translocation times of various $G\alpha_q$ constructs with different linkers or mutations were consistently between 17 and 20 s, when 200 nM rapamycin was applied (Figure S2). It should be noted that these times include all diffusion phenomena involved in the stimulation procedure, whereas the separation of $G\alpha_q$ and Gβγ dimers was recently reported to happen in less than 1 s (Adjobo-Hermans et al., 2011).

Additional constructs were coexpressed if necessary (FRET sensors, ECFP- or EGFP-$G\beta_1$ in experiments involving inducible $G\gamma_2$). In the inducible $G\gamma_2$ construct ($G\gamma_2$-FKBP-mRFP), the lysine-rich linker was included, and the CAAX box of $G\gamma_2$ was removed. It is worth noting that rapamycin-induced plasma membrane translocation of FKBP fusion of $G\gamma_2$ caused cotranslocation of $G\beta_1$ (Figure S1C).

Inducible $G\alpha_q$

Stimulation of HEK cells with ATP, a purinergic receptor agonist, resulted in a typical short calcium transient in a few cells followed by some sparse, additional transients (Figure 2A). Activation of constitutively active $G\alpha_q$ by 200 nM rapamycin induced a series of calcium spikes (Figure 2A), whereas treatment of the cells with DMSO or translocation of WT $G\alpha_q$ had no effect on $[Ca^{2+}]_i$ (data not shown). Moreover, plasma membrane translocation of GTPase-deficient $G\alpha_q$ constructs carrying additional mutations H218A or L254A that abolished the interaction of $G\alpha_q$ with PLCβ (Waldo et al., 2010) did not induce calcium oscillations (data not shown). This observation demonstrates the critical role of PLCβ in the generation of inducible $G\alpha_q$-evoked calcium transients. Potentially due to a lack in modulation by receptor desensitization and the lack of reassociation with Gβγ of the GTPase-deficient $G\alpha_q$ mutant, the calcium oscillations maintained their shape for extended periods of time (Figure 2B). Surprisingly, each cell showed a characteristic frequency as well as amplitude in its oscillatory behavior. The statistical analysis of peak frequencies, amplitudes, and peak durations is shown in Figure S3. None of the mentioned parameters of the induced calcium oscillations (i.e., frequency, amplitude, and peak duration) correlated with each other (data not shown). There was also a lack of correlation between any of the oscillation parameters and the initial cytoplasmic abundance of the FKBP fusion (before addition of rapamycin) or the loss of cytoplasmic FKBP fusion upon stimulation with the dimerizer (data not shown). This indicates that oscillation frequency and amplitude are governed by intrinsic cellular parameters rather than the exogenous manipulation. Median amplitude of calcium spikes after activation of the inducible $G\alpha_q$ is less than half of the one elicited by ATP (via endogenous P2Y receptors) when

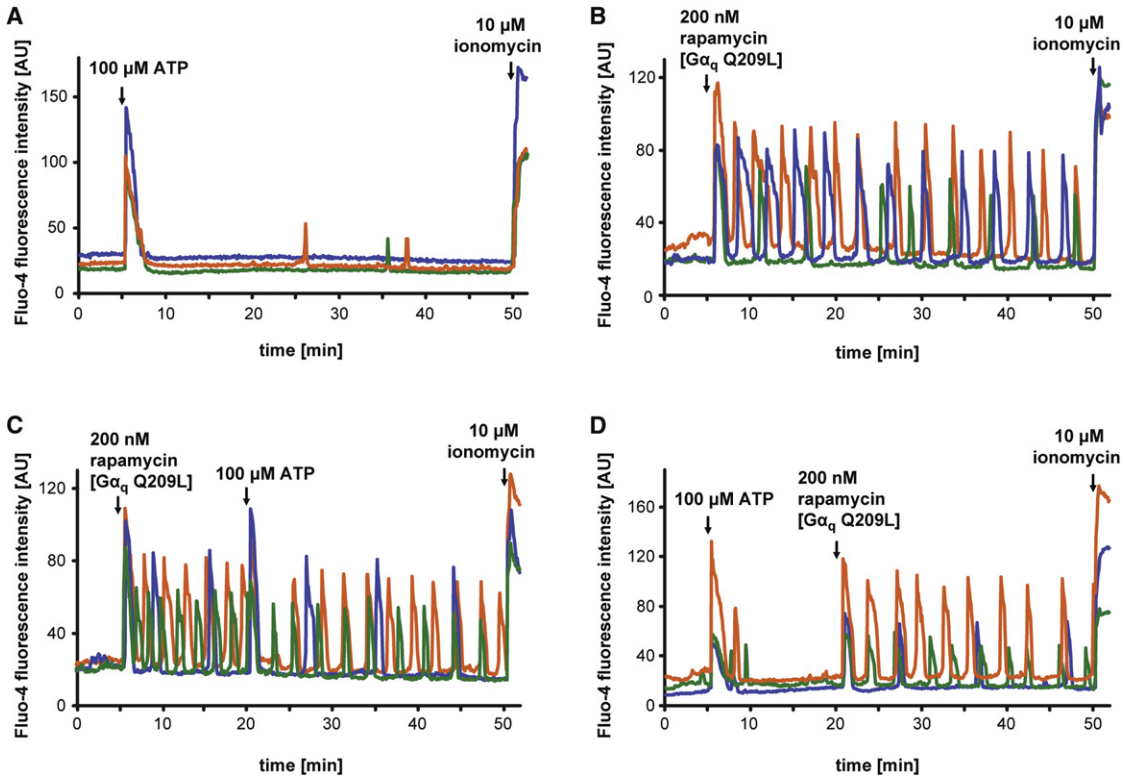

Figure 2. ATP-Evoked Calcium Transients and Calcium Oscillations Triggered by Inducible $G\alpha_q$ in HEK Cells

(A) Typical calcium traces upon stimulation with 100 µM ATP.

(B) Typical inducible $G\alpha_q$-evoked sustained calcium oscillations recorded in three individual cells. Some cells exhibited oscillations with a less-regular profile or produced only a single calcium transient.

(C) Calcium spiking continued after treating the cells with 100 µM ATP.

(D) Pretreatment with ATP did not affect calcium oscillations induced by rapamycin-dependent $G\alpha_q$.

See also Figures S2–S6.

averaged over more than 100 cells. Nevertheless, single-cell responses are frequently in the same range as those evoked by ATP.

The median onset of the response (defined as the time point when Fluo-4 fluorescence intensity exceeded 5× SD of the baseline) occurred 55 s after activation of the inducible $G\alpha_q$ (n = 131 cells) and 30 s after application of 100 µM ATP (n = 112 cells) (data not shown).

The effect of rapamycin could not be terminated by washing the cells, likely due to the high stability of the ternary FKBP-FRB-rapamycin complex (Figure S4).

Addition of ATP either several minutes after $G\alpha_q$ activation (Figure 2C) or before application of the drug (Figure 2D) did not modulate the oscillatory behavior. Inducing the calcium oscillations in the presence of extracellular manganese ions (Mn^{2+}) demonstrated rapid quenching of the Fluo-4 emission, indicating active calcium influx (store-operated calcium entry, SOCE) (Figure S5) triggered by emptying of intracellular calcium stores (Bird et al., 2008). To find out whether the calcium oscillations translated into a larger set of oscillating-signaling elements, we expressed MInsP-1, a FRET reporter that monitors *myo*-inositol 1,4,5-trisphosphate ($InsP_3$) levels, similar to that published by Sato et al. (2005). MInsP-1 showed a drop in FRET each time a calcium transient occurred (Figures 3A and 3B), indicating periodic modulation of PLC activity. With the same sensor we demonstrated that resting $InsP_3$ levels were not altered by expression of inducible $G\alpha_q$ components (Figure S6), suggesting that inducible $G\alpha_q$ does not exhibit basal activity before activation with rapamycin. It should be mentioned that the expression of the $InsP_3$ FRET sensor exhibited a buffering effect and reduced the number of cells showing rapamycin-induced calcium oscillations (data not shown).

PLC-activated hydrolysis of PIP_2 should lead to stimulation of protein kinase C (PKC) through the combined action of diacylglycerol and calcium (Newton, 2010). Therefore, we employed the plasma membrane-associated PKC-sensitive FRET reporter pmCKAR (Violin et al., 2003). Induction of $G\alpha_q$ produced distinct oscillations of PKC activity in individual cells (Figure 3C).

Validation of the $InsP_3$-Ca^{2+} Cross-Coupling Model

The mechanism by which inducible $G\alpha_q$-evoked calcium oscillations are best explained is the $InsP_3$-Ca^{2+} cross-coupling model (Harootunian et al., 1991; Meyer and Stryer, 1991; Politi et al., 2006) (see Figure 3D). The initial stimulation of PLCβ by $G\alpha_q$ induces the release of $InsP_3$. The subsequently elevated Ca^{2+} levels are needed to elicit full PLC activity in a feed-forward manner. The cycle is stopped when high $[Ca^{2+}]_i$ blocks the calcium-release function of the $InsP_3$ receptor ($InsP_3R$)

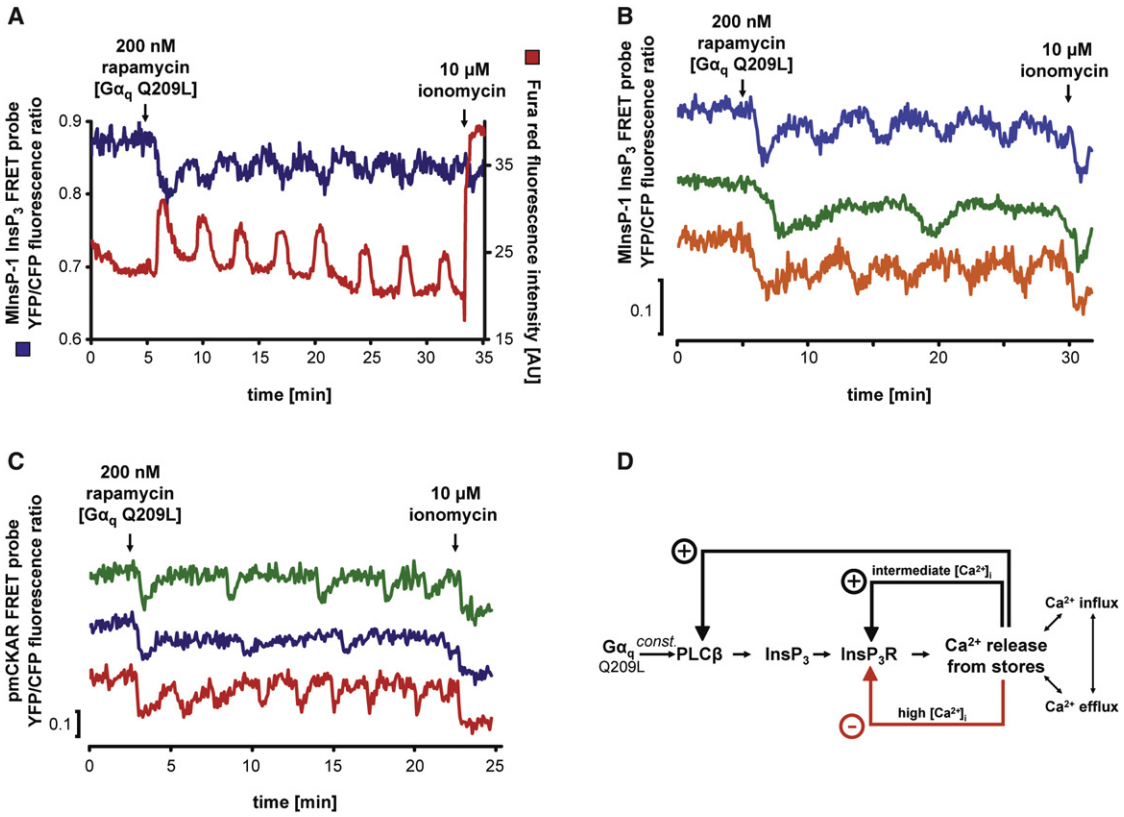

Figure 3. Effects of Inducible $G\alpha_q$ on Intracellular $InsP_3$ Levels and PKC Activity

(A) Simultaneous measurement of $InsP_3$ and calcium levels in the same cell revealed that every calcium spike was accompanied by an increase in cytosolic $InsP_3$ levels.

(B) Inducible $G\alpha_q$-evoked oscillations of $InsP_3$ levels recorded in the absence of calcium indicator demonstrated that oscillations of MInsP-1 fluorescence emission ratio shown in (A) were not an artifact of Fura red bleed through into the FRET channels. Traces have been arbitrarily offset for clarity.

(C) Oscillations of PKC activity evoked by inducible $G\alpha_q$. Traces have been arbitrarily offset for clarity.

(D) Schematic representation of the $InsP_3$-Ca^{2+} cross-coupling model of calcium oscillations. For details, see main text.

(Mikoshiba, 2007). Because Ca^{2+} efflux from internal stores ceases and the latter become refilled, SOCE stops, and remaining cytoplasmic Ca^{2+} is rapidly exported. The now reestablished low $[Ca^{2+}]_i$ leads to resensitization of the $InsP_3R$, thereby setting the stage for the next Ca^{2+} spike. We validated this model in experiments involving nonreceptor-mediated elevation of $[Ca^{2+}]_i$. When HEK cells were kept in nominally calcium-free medium, addition of the sarco/endoplasmic reticulum Ca^{2+} ATPase (SERCA) inhibitor thapsigargin (Putney, 2001) induced a transient calcium spike and a very weak and transient change in $InsP_3$ concentration (Figure 4A). When PLCβ was activated by $G\alpha_q$ prior to thapsigargin addition, an initial change in $InsP_3$ levels was observed in some cells, invariably followed by a strong $InsP_3$ transient after thapsigargin addition (Figure 4B). When calcium was added back to the medium, a massive increase in $[Ca^{2+}]_i$ and constantly elevated $InsP_3$ levels were observed (Figure 4B), explaining why calcium levels cannot oscillate after addition of thapsigargin. Quantitative comparison of the control cells and the cells expressing inducible $G\alpha_q$ revealed a significant difference in MInsP-1 FRET change upon calcium readdition to the thapsigargin-treated cells (Figure 4C). Control cells exhibited a median YFP/CFP emission ratio decrease of 1.75% (n = 60), whereas rapamycin-induced $G\alpha_q$ activity showed a median ratio decrease of 3.4% (n = 78, see Figure 4C). These results demonstrate that both $G\alpha_q$ and elevated $[Ca^{2+}]_i$ are crucial for full activation of PLC. Calcium itself is the major mediator of $[Ca^{2+}]_i$ oscillations because it governs its own release from internal stores and determines the rate of production of its mobilizing agent.

Inducible $G\alpha_s$

Next, we applied the chemical dimerizer approach to $G\alpha_s$, which is known to directly activate adenylate cyclase, thereby producing the second messenger cAMP from ATP (Sadana and Dessauer, 2009). Although we utilized constructs with an intact palmitoylation motif of $G\alpha_s$, the resulting fusion proteins exhibited cytosolic localization. Surprisingly, expression of constitutively active $G\alpha_s$ resulted in permanently elevated cAMP levels, as were measured with an Epac-based FRET sensor (Figure 5A). However, when WT $G\alpha_s$ fused to FKBP was expressed, addition of rapamycin generated a strong and sustained increase of cAMP levels (Figure 5A). We repeated this experiment with constructs devoid of the innate lipidation site of the GTPase and obtained analogous results (data not shown). We further examined the cytosolic FKBP fusions of $G\alpha_s$ in the absence of coexpressed FRB domains or the simple mRFP-$G\alpha_s$ constructs

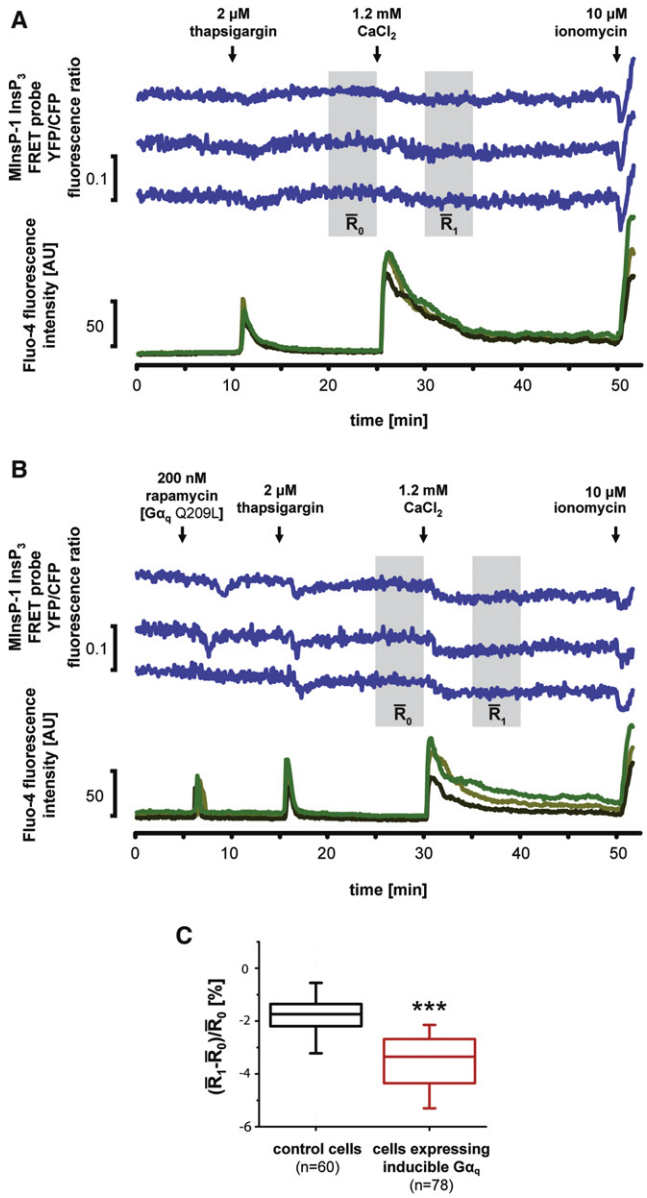

Figure 4. Effects of Nonreceptor-Mediated Elevation of $[Ca^{2+}]_i$ on Cytoplasmic $InsP_3$ Levels in HEK Cells

(A and B) Addition of thapsigargin to cells held in calcium-free medium caused transient elevation of $[Ca^{2+}]_i$. Upon calcium readdition a massive increase of cytosolic calcium levels was observed, followed by a prolonged period of elevated $[Ca^{2+}]_i$ (lower traces).

(A) In cells not expressing inducible $G\alpha_q$, sparse increases of $InsP_3$ concentration occurred during the time span of elevated calcium levels (upper traces).

(B) Activation of rapamycin-dependent $G\alpha_q$ in calcium-free medium evoked a single calcium spike in most of the cells (other cells did not respond at all) and a corresponding brief $InsP_3$ transient. Elevation of $[Ca^{2+}]_i$ led to a pronounced increase of $InsP_3$ levels (upper traces) indicating that active $G\alpha_q$ and calcium were both required for PLC activity. Presented calcium and $InsP_3$ traces were not recorded simultaneously. $InsP_3$ traces have been offset for clarity. Shaded boxes mark time frames before (R_0) and after calcium readdition (R_1) within which MInsP-1 emission ratio was averaged for calculations depicted in (C).

(C) Difference in emission ratio change between control and $G\alpha_q$-expressing cells is highly significant (Mann-Whitney *U* test, $U = 4003.0$; ***$p < 0.001$, two-tailed). Whiskers represent 10th and 90th percentile.

devoid of the lipidation site and found that the Q212L but not the WT forms still led to constantly high cAMP levels and, hence, exhibited basal activity (Figure S7). It appears that any constantly active cytoplasmic fusion of $G\alpha_s$ Q212L will be able to activate adenylate cyclase in a kiss-and-run fashion, potentially due to a high intrinsic affinity.

This novel method of activating intracellular cAMP production complements the commonly used direct activation of adenylate cyclase with forskolin (Ponsioen et al., 2004; Sadana and Dessauer, 2009). Inducible $G\alpha_s$ will lead to elevated cAMP levels only in those cells expressing both protein components of the inducible system, thus permitting the observation of activated versus silent cells in one experiment. Importantly, contrary to the forskolin approach, rapamycin-dependent $G\alpha_s$ has a potential of being applicable in vivo because cAMP levels could be selectively elevated in a chosen organ or cell type (given tissue-specific expression of all protein components of the inducible system).

Crosstalk of Calcium and cAMP Signaling

In order to make use of the rapamycin-inducible $G\alpha$ protein constructs, we investigated the crosstalk of calcium- and cAMP-mediated signaling by monitoring $[Ca^{2+}]_i$. In HEK cells, induction of cAMP levels by rapamycin-dependent $G\alpha_s$ in combination with purinergic stimulation by ATP generated secondary calcium transients independent of the order of stimuli (Figures 5B and 5C). It was previously suggested that increased cAMP levels have a potentiating effect on calcium transients in HEK cells (Schmidt et al., 2001). We find that in our experimental setup calcium oscillations were induced via PKA and not by Epac, another cAMP effector (Holz et al., 2008). This was demonstrated by generating oscillations with the membrane-permeant acetoxymethyl (AM) ester of the PKA-selective agonist 6-benzyl-cAMP (6-Bz-cAMP/AM, see Figure S8A), whereas the Epac-selective agonist 8-*p*-chlorophenylthio-2′-O-methyl-cAMP/AM (8-pCPT-2′-O-Me-cAMP/AM) (Ponsioen et al., 2004; Holz et al., 2008) had a negligible effect (Figure S8B). We chose to test 2 µM concentration of both cAMP analogs because application of 2 µM 8-pCPT-2′-O-Me-cAMP/AM resulted in saturation of the Epac-based cAMP FRET sensor (Figure S9A), whereas 1 µM concentration of this compound elicited a submaximal response (Figure S9B). A total of 2 µM 6-Bz-cAMP/AM had no effect on the FRET levels of the Epac-based sensor (Figure S9C). Instead of rapamycin-induced $G\alpha_s$ stimulation, an increase of cAMP levels by the β-adrenergic agonist isoprenaline generated calcium oscillations in a similar manner (Figures S8C and S8D). Interestingly, the constant presence of ATP was required for the isoprenaline-induced oscillations because treatment of the cells with apyrase, an enzyme that rapidly hydrolyzes ATP, resulted in full abolishment of calcium oscillations (Figure S8E). Calcium oscillations following rapamycin-induced $G\alpha_q$ translocation were strongly affected by addition of isoprenaline resulting in increased calcium levels followed by faster calcium oscillations (Figures S8F and S8G). Similarly, also calcium transients evoked by muscarinic stimulation of HEK cells with carbachol were potentiated by isoprenaline (Figures S8H and S8I). These results suggest that cAMP signaling is not acting on the purinergic receptor level as was indicated by the apyrase experiment. The most plausible explanation of the observed phenomenon relates to the reported sensitization of the $InsP_3R$

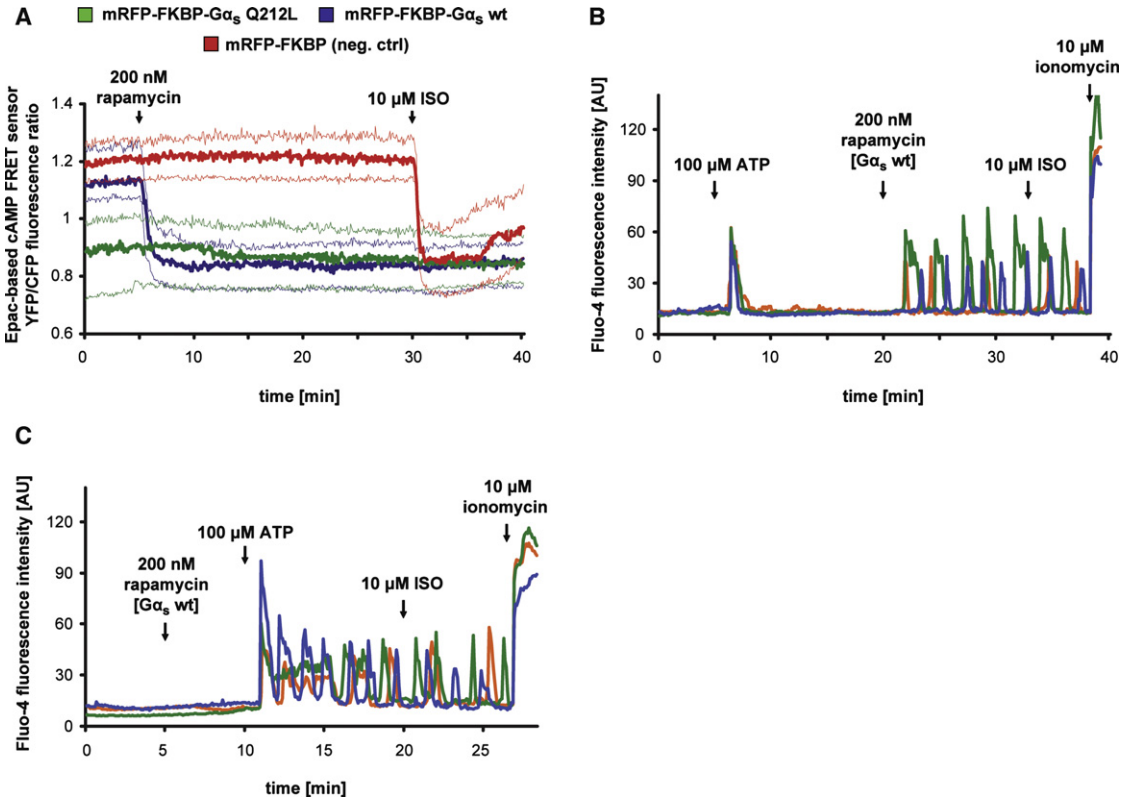

Figure 5. Effects of Inducible $G\alpha_s$ in HEK Cells

(A) Plasma membrane translocation of WT $G\alpha_s$ (blue trace) resulted in sustained elevation of cAMP levels as measured by an Epac-based sensor. Cells expressing FKBP fusion of a GTPase-deficient $G\alpha_s$ mutant exhibited constantly elevated cAMP levels (green trace). Plasma membrane translocation of the negative control construct (mRFP-FKBP) had no effect on cAMP levels (red trace). Bold traces represent the median value of 3 independent experiments (30–40 cells); thin traces represent quartile distance.

(B and C) Influence of rapamycin/$G\alpha_s$-induced elevated cAMP levels on ATP-evoked calcium signaling. Calcium oscillations were triggered regardless of the addition sequence, whereas rapamycin addition had no effect on its own. Addition of isoprenaline (ISO) had no further effect on calcium oscillations.

See also Figures S7–S9.

for lower $InsP_3$ levels upon phosphorylation by PKA (Mikoshiba, 2007; Bruce et al., 2002; Wagner et al., 2003). Under these conditions subthreshold levels of $InsP_3$ generated by the desensitized purinergic receptor might become sufficient to elicit pronounced calcium transients.

Modulation of Calcium Transients by Inducible $G\beta_1\gamma_2$

An apparently similar effect to the aforementioned cAMP-evoked potentiation of calcium signaling (i.e., generation of secondary calcium transients) was observed when a FKBP-fused $G\gamma_2$ was activated via the rapamycin system. Although translocation of $G\beta_1\gamma_2$ to the plasma membrane had no direct effect on intracellular cAMP levels (data not shown), we observed the onset of massive calcium oscillations when the $G\beta_1\gamma_2$ translocation was induced in the presence of ATP (Figures S8J and S8K). It should be noted that treatment of HEK cells with apyrase prior to the inducible $G\beta_1\gamma_2$ activation vastly abrogated any calcium transients (data not shown). We suspect a direct effect of $G\beta_1\gamma_2$ on PLCβ activity (Wettschureck and Offermanns, 2005; Waldo et al., 2010; Suh et al., 2008; Smrcka, 2008). However, it seems that in the majority of the cases, $G\beta_1\gamma_2$ alone is insufficient for full activation of the enzyme. $G\beta_1\gamma_2$ may rather play a role in modulation of calcium transients or sensitization of cells for subthreshold levels of calcium-mobilizing agonists. Further work aiming at a closer characterization of the observed phenomena is currently in progress.

SIGNIFICANCE

We generated rapamycin-inducible functional fusion proteins for two of the most prominent heterotrimeric G protein α subunits as well as the $G\beta_1\gamma_2$ dimer. Unlike with any other method, it is now possible to activate G protein subunits independently. For the first time, a "pure" $G\alpha_q$, $G\alpha_q$, or $G\beta_1\gamma_2$ signal may be produced. Our approach is expected to be independent from endogenous trimeric G protein levels as we overexpress the activatable subunit. We demonstrated that this dissection of the signaling network leads in case of $G\alpha_q$ to an unusual form of calcium oscillations. This is likely due to lack of interference at the G protein level. Because the onset of activity is fast, cellular effects may be manipulated within subminute resolution, sufficiently fast for events in nonexcitable cells. Even faster manipulations, i.e., in neurons, would require application of light-sensitive

tools (Janovjak et al., 2010). The probes permit studying the relative contribution of each subunit in living cells and in the future potentially also in entire organisms. Spatially restricted activation might be achieved by using photoactivatable rapamycin derivatives in the future (Umeda et al., 2011).

The continuous activation of PLCβ by $G\alpha_q$ leads to the activation of a basic, intrinsic oscillatory machinery involving PLC activity and $InsP_3$ and intracellular calcium levels that in turn triggers oscillatory PKC activity. Interestingly, each cell in the dish seems to be equipped with a unique composition of the oscillation-relevant molecules, as is suggested by the complete absence of correlation between signal durations, intensities, frequencies, and expression levels. The individual calcium response patterns of neighboring cells might have important consequences for physiological cell function, and therefore, these regular unmodulated calcium oscillations should be studied in intact tissue.

EXPERIMENTAL PROCEDURES

DNA Constructs' Design

All constructs were cloned in the standard pEGFP vector backbone (Clontech). Site-directed mutagenesis was performed using QuikChange Lightning Site-Directed Mutagenesis Kit (Stratagene) according to the manufacturer's protocol.

The plasma membrane-anchored rapamycin-binding domain consists of the N-terminal plasma membrane-targeting peptide of rat Lck kinase (aa 1–10), FRB T2098L domain (aa 2021–2113 of human mTOR), and ECFP, either nonmodified or as an ECFP W66A nonfluorescent mutant. The linker between the signaling peptide and FRB consists of the aa sequence RSANSGAGAGA GAILSR. The linker between FRB and ECFP is TSYPYD-VPDYAPVAT.

FKBP fusions of the Gα subunits of the heterotrimeric G proteins consist of mRFP, human FKBP1A, and a full-length sequence of the corresponding human Gα subunit. The linker between mRFP and FKBP is SGLRSRAAA-GAGGAARAA. In the functional $G\alpha_q$ construct with the lysine-rich linker, the aa sequence between FKBP and $G\alpha_q$ is ARGAAAGAGGAGRS**GKKGKK GKK**GTT. In two other nonfunctional variants of this construct, the sequences of the latter linker are ARGAAAGAGGAGRS**GGKL**GTT and ARGAAAGAGG AGRS-**GGAGGAGGA**GTT. All constructs with $G\alpha_q$ fused to FKBP contain C9S, C10S substitutions. Additional mutations of $G\alpha_q$ (Q209L, H218A, L254A) were introduced by site-directed mutagenesis.

In the FKBP-$G\alpha_s$ fusion constructs, $G\alpha_s$ is connected with the rapamycin-binding domain by the lysine-rich linker (see above). cDNA of $G\alpha_s$ (isoform f according to the nomenclature of Entrez Gene database, http://www.ncbi.nlm.nih.gov/gene) was obtained from ImaGenes (clone name IRAUp969F0240D) and converted into isoform g (Entrez Gene) by site-directed mutagenesis. GTPase-deficient $G\alpha_s$ Q212L was generated by site-directed mutagenesis. C3S mutants of the FKBP fusion constructs of $G\alpha_s$ and the respective mRFP-$G\alpha_s$ C3S constructs were generated by site-directed mutagenesis. The linker between mRFP and the GTPase in the latter fusions was SGLRSRSAAAGAGG.

The construct used as a negative control of rapamycin-induced plasma membrane translocation events consists only of mRFP and FKBP, linked as described above. FKBP is followed by ARGAAAGAGGAGR and a stop codon.

Inducible $G\gamma_2$ consists of human $G\gamma_2$ (aa 1–67), FKBP, and mRFP. The linker between $G\gamma_2$ and FKBP is SRSKKGKKGKKGRSRSAAAGAGGAARAA. FKBP and mRFP are connected by ARGAAAGAGGAGRSGGAGGAGGAGT. ECFP and EGFP fusions of human $G\beta_1$ contain respective fluorescent proteins linked to the $G\beta_1$ subunit via an SGLRSRAQASNS linker.

MInsP-1 contains a C-terminally truncated ECFP (aa 1–227) connected by a 2 aa-linker (TG) to the $InsP_3$-binding pocket of human $InsP_3R1$ (aa 224–579), the latter being linked by 2 aa (TR) to cp172Venus. cDNA of $InsP_3R1$ was generated from total RNA isolated from the HeLa CCL-2 cell line (RNeasy Kit; QIAGEN) using RevertAid Premium First Strand cDNA Synthesis Kit (Fermantas) with an oligo$(dT)_{18}$ primer according to the manufacturer's protocol.

Cell Culture and Transfection

All cell experiments, except for the rapamycin washout, were performed with HEK293 cells. HEK cells were grown in DMEM containing 4.5 g/l glucose, supplemented with 10% FBS, 1 mM sodium pyruvate, and 0.1 mg/ml Primocin. HeLa CCL-2 cells were grown in DMEM containing 1 g/l glucose, supplemented with 10% FBS and 0.1 mg/ml Primocin. For live-imaging experiments, HEK cells were plated in 35 mm diameter μ-Dish with ibiTreat surface (ibidi). HeLa cells were plated in gridded glass-bottom dishes (MatTek). Cells were transfected at around 70% confluency with Lipofectamine 2000 reagent. Transfections were performed in DMEM containing 4.5 g/l glucose without any other supplements (HEK) or OptiMem (HeLa) according to the manufacturer's instructions. Cells were used 18–30 hr after transfection. For consistency of the culturing conditions, HEK cells without transfection were also incubated in DMEM without supplements for 18–30 hr before imaging.

For experiments involving monitoring of cytosolic calcium levels, the cells were loaded with Fluo-4/AM or Fura red/AM (1 μg/ml, directly in the transfection medium for 20 min at 37°C [HEK] or at room temperature [HeLa]). Five minute Fluo-4 loading of HEK cells was performed for experiments aiming at quantitative analysis of calcium transients. After loading with the calcium indicator, the medium was gently exchanged with the imaging medium (without a washing step). Standard imaging medium contained 20 mM HEPES (pH 7.4), 115 mM NaCl, 1.2 mM $CaCl_2$, 1.2 mM $MgCl_2$, 1.2 mM K_2HPO_4, and 2 g/l glucose. In calcium-free imaging medium $CaCl_2$ was omitted, and the medium was supplemented with 0.1 mM EGTA.

Stock solutions of all chemical compounds added to the cells, either before or during the live-imaging time-lapse, were prediluted in imaging medium before their careful addition to the dish. Cells were incubated at 37°C in the environmental chamber of the microscope for about 15 min before image acquisition.

Microscopy, Image Processing, and Analysis

All experiments, except for the rapamycin washout experiments (HeLa cells, 22°C), were performed on a Leica TCS SP2 AOBS confocal microscope in an environmental chamber at 37°C. For monitoring of intracellular calcium levels and FRET measurements, an HCX PL APO lbd.BL 40.0× 1.40 oil objective was used. The pinhole was fully opened. Images were acquired in 8 bit mode, with two to four line averaging and 5 s between frames.

In calcium-imaging experiments Fluo-4 and Fura red were excited with the 488 and 405 nm laser lines, respectively, and their emission was sampled from 510 to 600 nm and from 625 to 725 nm, respectively.

For CFP/YFP FRET measurements the 405 nm laser was used for excitation of CFP. Donor emission was sampled between 470 and 510 nm, acceptor emission between 520 and 540 nm. Excitation and emission settings were kept constant for ratiometric FRET analysis in order to image cells expressing similar amounts of the sensors and avoid expression-related variability.

In experiments involving simultaneous measurement of intracellular calcium and $InsP_3$ levels, images of both donor and acceptor of MInsP-1 were corrected for the Fura red bleed through before ratio calculation.

Image processing was performed using ImageJ (http://rsb.info.nih.gov/ij); further calculations were performed in Microsoft Office Excel and Origin. Computational analysis of calcium oscillation patterns was performed in a custom-written Perl script developed by Jean-Karim Hériché (EMBL Heidelberg, Heidelberg, Germany). The Mann-Whitney *U* test was performed online: http://elegans.swmed.edu/~leon/stats/utest.html. In FRET experiments background levels were measured outside the cells and subtracted globally. The median filter (1 pixel) was used for image smoothening. A threshold was applied before calculation of acceptor/donor ratio or FRET efficiency.

In time-lapse microscopy analysis, individual cell traces were obtained. Every experiment was performed at least three times. Data presented for every experiment are representative of at least 30 cells, except for experiments involving MInsP-1 FRET probe, where data are representative of 10 cells or more.

SUPPLEMENTAL INFORMATION

Supplemental Information includes nine figures and one table and can be found with this article online at doi:10.1016/j.chembiol.2011.07.013.

ACKNOWLEDGMENTS

We are grateful to Jean-Karim Hériché (EMBL Heidelberg, Heidelberg, Germany) for his support in computational analysis of calcium oscillation patterns. We thank Tamás Balla (NIH, Bethesda, MD, USA) for rapamycin-binding domains, Kees Jalink (NCI, Amsterdam) for the Epac-based cAMP FRET sensor, Theodorus Gadella (University of Amsterdam, Amsterdam) for cDNA of $G\alpha_q$, $G\beta_1$, and $G\gamma_2$, Alexandra Newton (University of California San Diego, La Jolla, CA, USA) for pmCKAR, Alen Piljić and Gregor Reither (EMBL Heidelberg) for technical advice, Heike Stichnoth (EMBL Heidelberg) for cultured cells, and Tobias Meyer (Stanford University, Stanford, CA, USA.) for critical reading of the initial manuscript. This work was supported by the Helmholtz Association (SBCancer), and the ESF and the DFG (Schu 943/8-1).

Received: April 20, 2011
Revised: June 28, 2011
Accepted: July 12, 2011
Published: September 22, 2011

REFERENCES

Adjobo-Hermans, M.J., Goedhart, J., van Weeren, L., Nijmeijer, S., Manders, E.M., Offermanns, S., and Gadella, T.W., Jr. (2011). Real-time visualization of heterotrimeric G protein Gq activation in living cells. BMC Biol. *9*, 32.

Bird, G.S., DeHaven, W.I., Smyth, J.T., and Putney, J.W., Jr. (2008). Methods for studying store-operated calcium entry. Methods *46*, 204–212.

Bruce, J.I., Shuttleworth, T.J., Giovannucci, D.R., and Yule, D.I. (2002). Phosphorylation of inositol 1,4,5-trisphosphate receptors in parotid acinar cells. A mechanism for the synergistic effects of cAMP on Ca^{2+} signaling. J. Biol. Chem. *277*, 1340–1348.

Fili, N., Calleja, V., Woscholski, R., Parker, P.J., and Larijani, B. (2006). Compartmental signal modulation: endosomal phosphatidylinositol 3-phosphate controls endosome morphology and selective cargo sorting. Proc. Natl. Acad. Sci. USA *103*, 15473–15478.

Harootunian, A.T., Kao, J.P., Paranjape, S., and Tsien, R.Y. (1991). Generation of calcium oscillations in fibroblasts by positive feedback between calcium and IP_3. Science *251*, 75–78.

Holz, G.G., Chepurny, O.G., and Schwede, F. (2008). Epac-selective cAMP analogs: new tools with which to evaluate the signal transduction properties of cAMP-regulated guanine nucleotide exchange factors. Cell. Signal. *20*, 10–20.

Inoue, T., Heo, W.D., Grimley, J.S., Wandless, T.J., and Meyer, T. (2005). An inducible translocation strategy to rapidly activate and inhibit small GTPase signaling pathways. Nat. Methods *2*, 415–418.

Janovjak, H., Szobota, S., Wyart, C., Trauner, D., and Isacoff, E.Y. (2010). A light-gated, potassium-selective glutamate receptor for the optical inhibition of neuronal firing. Nat. Neurosci. *13*, 1027–1032.

Karginov, A.V., Ding, F., Kota, P., Dokholyan, N.V., and Hahn, K.M. (2010). Engineered allosteric activation of kinases in living cells. Nat. Biotechnol. *28*, 743–747.

Laketa, V., Zarbakhsh, S., Morbier, E., Subramanian, D., Dinkel, C., Brumbaugh, J., Zimmermann, P., Pepperkok, R., and Schultz, C. (2009). Membrane-permeant phosphoinositide derivatives as modulators of growth factor signaling and neurite outgrowth. Chem. Biol. *16*, 1190–1196.

Meyer, T., and Stryer, L. (1991). Calcium spiking. Annu. Rev. Biophys. Biophys. Chem. *20*, 153–174.

Mikoshiba, K. (2007). IP_3 receptor/Ca^{2+} channel: from discovery to new signaling concepts. J. Neurochem. *102*, 1426–1446.

Newton, A.C. (2010). Protein kinase C: poised to signal. Am. J. Physiol. Endocrinol. Metab. *298*, E395–E402.

Politi, A., Gaspers, L.D., Thomas, A.P., and Höfer, T. (2006). Models of IP_3 and Ca^{2+} oscillations: frequency encoding and identification of underlying feedbacks. Biophys. J. *90*, 3120–3133.

Ponsioen, B., Zhao, J., Riedl, J., Zwartkruis, F., van der Krogt, G., Zaccolo, M., Moolenaar, W.H., Bos, J.L., and Jalink, K. (2004). Detecting cAMP-induced Epac activation by fluorescence resonance energy transfer: Epac as a novel cAMP indicator. EMBO Rep. *5*, 1176–1180.

Putney, J.W., Jr. (2001). Pharmacology of capacitative calcium entry. Mol. Interv. *1*, 84–94.

Sadana, R., and Dessauer, C.W. (2009). Physiological roles for G protein-regulated adenylyl cyclase isoforms: insights from knockout and overexpression studies. Neurosignals *17*, 5–22.

Sato, M., Ueda, Y., Shibuya, M., and Umezawa, Y. (2005). Locating inositol 1,4,5-trisphosphate in the nucleus and neuronal dendrites with genetically encoded fluorescent indicators. Anal. Chem. *77*, 4751–4758.

Schmidt, M., Evellin, S., Weernink, P.A., von Dorp, F., Rehmann, H., Lomasney, J.W., and Jakobs, K.H. (2001). A new phospholipase-C-calcium signalling pathway mediated by cyclic AMP and a Rap GTPase. Nat. Cell Biol. *3*, 1020–1024.

Schultz, C., Vajanaphanich, M., Harootunian, A.T., Sammak, P.J., Barrett, K.E., and Tsien, R.Y. (1993). Acetoxymethyl esters of phosphates, enhancement of the permeability and potency of cAMP. J. Biol. Chem. *268*, 6316–6322.

Shokat, K., and Velleca, M. (2002). Novel chemical genetic approaches to the discovery of signal transduction inhibitors. Drug Discov. Today *7*, 872–879.

Smrcka, A.V. (2008). G protein betagamma subunits: central mediators of G protein-coupled receptor signaling. Cell. Mol. Life Sci. *65*, 2191–2214.

Subramanian, D., Laketa, V., Müller, R., Tischer, C., Zarbakhsh, S., Pepperkok, R., and Schultz, C. (2010). Activation of membrane-permeant caged PtdIns(3) P induces endosomal fusion in cells. Nat. Chem. Biol. *6*, 324–326.

Suh, B.C., Inoue, T., Meyer, T., and Hille, B. (2006). Rapid chemically induced changes of PtdIns(4,5)P2 gate KCNQ ion channels. Science *314*, 1454–1457.

Suh, P.G., Park, J.I., Manzoli, L., Cocco, L., Peak, J.C., Katan, M., Fukami, K., Kataoka, T., Yun, S., and Ryu, S.H. (2008). Multiple roles of phosphoinositide-specific phospholipase C isozymes. BMB Rep *41*, 415–434.

Szentpetery, Z., Várnai, P., and Balla, T. (2010). Acute manipulation of Golgi phosphoinositides to assess their importance in cellular trafficking and signaling. Proc. Natl. Acad. Sci. USA *107*, 8225–8230.

Terrillon, S., and Bouvier, M. (2004). Receptor activity-independent recruitment of betaarrestin2 reveals specific signalling modes. EMBO J. *23*, 3950–3961.

Umeda, N., Ueno, T., Pohlmeyer, C., Nagano, T., and Inoue, T. (2011). A photocleavable rapamycin conjugate for spatiotemporal control of small GTPase activity. J. Am. Chem. Soc. *133*, 12–14.

Varnai, P., Thyagarajan, B., Rohacs, T., and Balla, T. (2006). Rapidly inducible changes in phosphatidylinositol 4,5-bisphosphate levels influence multiple regulatory functions of the lipid in intact living cells. J. Cell Biol. *175*, 377–382.

Violin, J.D., Zhang, J., Tsien, R.Y., and Newton, A.C. (2003). A genetically encoded fluorescent reporter reveals oscillatory phosphorylation by protein kinase C. J. Cell Biol. *161*, 899–909.

Wagner, L.E., 2nd, Li, W.H., and Yule, D.I. (2003). Phosphorylation of type-1 inositol 1,4,5-trisphosphate receptors by cyclic nucleotide-dependent protein kinases: a mutational analysis of the functionally important sites in the $S2^+$ and $S2^-$ splice variants. J. Biol. Chem. *278*, 45811–45817.

Waldo, G.L., Ricks, T.K., Hicks, S.N., Cheever, M.L., Kawano, T., Tsuboi, K., Wang, X., Montell, C., Kozasa, T., Sondek, J., and Harden, T.K. (2010). Kinetic scaffolding mediated by a phospholipase C-β and G_q signaling complex. Science *330*, 974–980.

Wettschureck, N., and Offermanns, S. (2005). Mammalian G proteins and their cell type specific functions. Physiol. Rev. *85*, 1159–1204.

Wu, Y.I., Frey, D., Lungu, O.I., Jaehrig, A., Schlichting, I., Kuhlman, B., and Hahn, K.M. (2009). A genetically encoded photoactivatable Rac controls the motility of living cells. Nature *461*, 104–108.

